Separation Science and Technology
Publication details, including instructions for authors and subscription information:
http://www.informaworld.com/smpp/title~content=t713708471

Lysine Adsorption on Cation Exchange Resin. III. Multicolumn Adsorption/Desorption Operation

Hidetada Nagai[ab]; Giorgio Carta[a]
[a] Department of Chemical Engineering, University of Virginia, Charlottesville, Virginia, USA [b] Technology and Engineering Laboratory, Ajinomoto, Co., Inc., Kawasaki-ku, Kawasaki-shi, Japan

To cite this Article Nagai, Hidetada and Carta, Giorgio(2005) 'Lysine Adsorption on Cation Exchange Resin. III. Multicolumn Adsorption/Desorption Operation', Separation Science and Technology, 40: 4, 791 — 809
To link to this Article: DOI: 10.1081/SS-200041099
URL: http://dx.doi.org/10.1081/SS-200041099

Separation Science and Technology, 40: 791–809, 2005

ISSN 0149-6395 print/1520-5754 online
DOI: 10.1081/SS-200041099

Lysine Adsorption on Cation Exchange Resin. III. Multicolumn Adsorption/ Desorption Operation

Hidetada Nagai
Department of Chemical Engineering, University of Virginia, Charlottesville, Virginia, USA and Ajinomoto, Co., Inc., Technology and Engineering Laboratory, Kawasaki-ku, Kawasaki-shi, Japan

Giorgio Carta
Department of Chemical Engineering, University of Virginia, Charlottesville, Virginia, USA

Abstract: A model previously developed to describe ion exchange equilibria, kinetics, and column dynamics of lysine adsorption on a strong acid cation exchanger is extended to simulate the cyclic adsorption/desorption of lysine in a multicolumn, simulated countercurrent system. The system simulated comprises an adsorption zone, a desorption zone, and two zones where unadsorbed feed components and excess desorbent are removed. Multiple columns are distributed among the four zones in different simulated countercurrent schemes, including a scheme that allows recycling of excess desorbent and another where the lysine recovery yield is enhanced at low flow rates by lowering the pH in the last column of the adsorption zone. Model predictions are validated by comparison with experimental results obtained in an eight-column bench scale apparatus and a parametric study is conducted with the model to determine the effects of critical design variables.

Keywords: Equilibria, kinetics, column dynamics, lysine adsorption, ion exchange

Received March 2, 2004, Accepted September 14, 2004.
This research was supported by Ajinomoto Co., Inc.
Address correspondence to Giorgio Carta, Department of Chemical Engineering, University of Virginia, Charlottesville, VA, USA. E-mail: gc@virginia.edu

INTRODUCTION

In our prior work (1, 2), we examined the equilibrium and kinetics of lysine ion exchange on a strong acid, styrene-divinylbenzene cation exchanger and the column dynamic behavior. Lysine possesses a basic side chain. As a result lysine adsorption occurs via the stoichiometric exchange of divalent lysine cations, monovalent lysine cations, or a combination of both, depending on the composition of the solution. The lysine adsorption isotherm, thus, has a complex shape that results in complicated column dynamics. At low-feed pH, when the divalent form is dominant, the lysine breakthrough curve behaves like a shock, since ion exchange of divalent lysine is favorable. Conversely, at high-feed pH, when the monovalent form of lysine is dominant, the breakthrough curve is gradual and exhibits simple wave behavior due to the unfavorable nature of monovalent lysine cation exchange. Finally, at intermediate feed pH values, the breakthrough curve exhibits a gradual portion followed by a shock. The mass transfer kinetics, which control the rate of ion exchange, were also studied; and a model based on the Nernst-Planck formulation was used to describe batch adsorption and desorption. A film model approximation of the Nernst-Planck model was developed to quantitatively predict the lysine breakthrough behavior as well as lysine desorption with ammonium hydroxide. The latter case is completely mass transfer controlled, since the negatively charged form of lysine, dominant at pH greater than 11, is excluded from the cation exchange resin. Thus, equilibrium is no longer limiting and complete desorption is attainable. On the other hand, the rate of desorption is diffusion controlled and is generally slow because of the small diffusivity of lysine cations in the resin. As a result, the desorption curve has a pronounced tail, which has a significant impact on productivity and desorbent consumption.

Industrial application of ion exchange for the recovery and separation of amino acids is often carried out in multicolumn systems (3, 4). Using a cation exchanger, amino acids, such as lysine, can be loaded at a low pH, where they are favorably adsorbed, and desorbed with an alkaline solution that raises the pH to a value where the amino acid becomes negatively charged. In a multicolumn system, the breakthrough capacity can be increased by staging the columns in a simulated moving bed arrangement. Moreover, the desorbent consumption can be reduced since the high pH effluent from a desorption column can be fed to another column in series providing further contact with lysine loaded resin.

Simulated moving bed systems have been used extensively for various applications including the separation of xylenes (5), the separation of glucose-fructose mixtures (6), the separation of phenylalanine/tyrosine mixtures (7), and numerous chiral separations (e.g., 8–10). These separations are based on relatively small differences in adsorption affinity and are usually operated close to local equilibrium conditions. Methodologies for the design of these systems

have also been developed (e.g., 11–14). In most cases, the starting point is a local equilibrium analysis, which is then extended to account for mass transfer effects.

Multicolumn systems for lysine recovery, on the other hand, are different in scope from the more common applications of simulated moving bed systems. The primary objective is to recover lysine from largely nonadsorbed fermentation broth components by adsorbing cationic lysine on a cation exchange resin, followed by elution with base. The product is the free base-form of lysine, which can then be subjected to further purification and eventually crystallization. The process efficiency is a strong function of the uptake capacity and the rate of adsorption and desorption as well as the configuration of the process. Thus, a model taking onto account these factors is desirable for process design and optimization.

Several different multicolumn process schemes could be used. The ones considered in this work are shown in Fig. 1. The process schemes shown comprise eight columns, although any number could be used distributed among the different zones. As shown, the columns are arranged in four separate zones supplied with the lysine feed (F), the desorbent (D), and two rinse streams (R1 and R2). The columns are rotated in progression from right to left at periodic time intervals. With reference to Fig. 1A, the process functions as follows. The columns in positions 1 to 3 are supplied with the lysine feed and are connected in series. This series arrangement allows a more efficient containment of the mass transfer zone. If a single column were used for loading, regeneration would have to occur before the adsorption capacity is utilized to a large extent. Conversely, by using two or more columns in series, only the first column is regenerated at each step, allowing a more efficient utilization of the ion exchange capacity. The columns in positions 5–7 are supplied with the ammonium hydroxide desorbent. These columns are also connected in a series. Since a long desorption tail is expected as a result of the slow diffusion of lysine in the resin (2), a better utilization of the desorbent stream can be obtained by allowing the alkaline effluent from each column to flow into the next one. Since the amount of lysine desorbed at high pH is largely dependent only on the time of exposure to the ammonium hydroxide solution, a greater amount of lysine can be desorbed in this manner. Finally, there is one column in position 4 and one in position 8. The column in position 4 is purged of the excess ammonium hydroxide remaining in the column interstices prior to moving it to the feed loading train (positions 1–3), while the column in position 8 is purged of the unbound fermentation broth contaminants prior to moving it to the lysine recovery train (positions 5–7).

Figures 1B and 1C show two alternative configurations. In the first of these, the effluent leaving the R1 rinse column is combined with the desorbent stream to reduce the consumption of ammonia by recycling the ammonia left in the column interstices after desorption. In the second scheme (Fig. 1C), the effluent from the column in position 2 is acidified to convert lysine to its divalent cationic form. This way, the first two columns

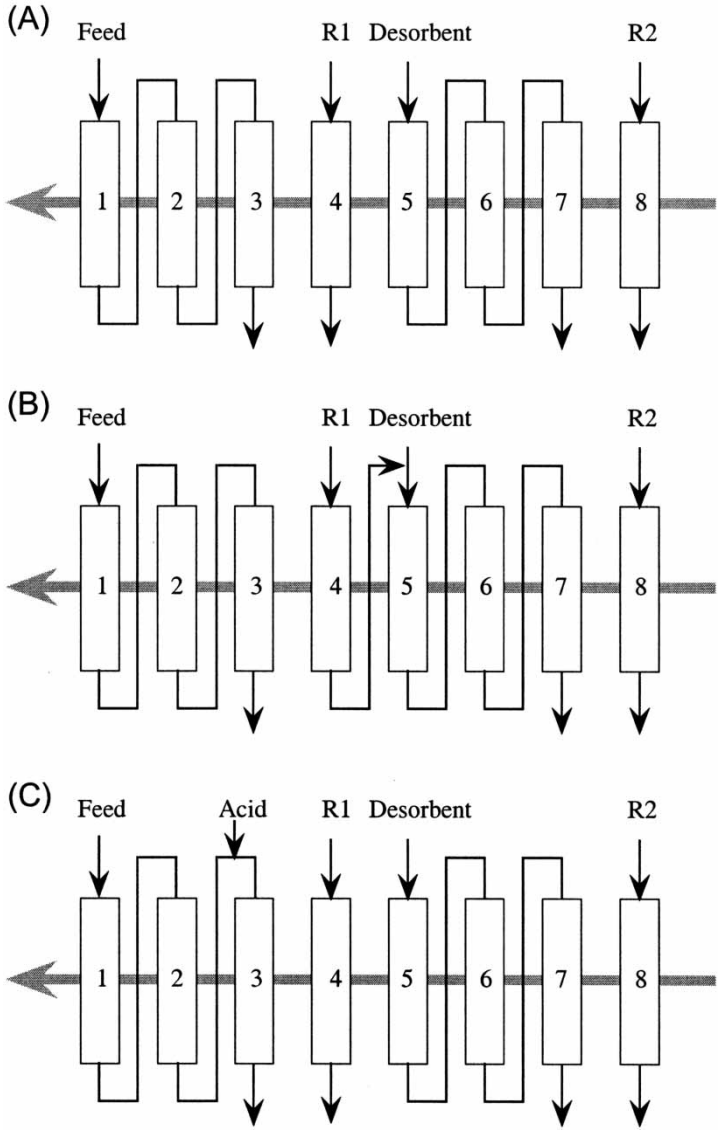

Figure 1. Configurations for the multicolumn lysine recovery process. The gray arrows show the direction of column rotation.

in the adsorption train can be loaded with monovalent lysine, which results in high capacity, but a broad mass transfer zone, while the last column serves as a final capture step where divalent lysine is loaded with a sharper mass transfer zone, but lower capacity.

Obviously, a large number of parameters need to be considered to arrive at an optimum design. As a result, in this work we consider the application of a mass transfer model to describe these operations. The model based on equilibrium and rate determinations made in our prior work (1, 2), is validated for multicolumn operation by comparison with experimental results obtained with a bench scale apparatus. The effects of various operating parameters are then determined by numerical simulation.

MATERIALS AND METHODS

The resin used in this work is Dowex HCR-W2 (Dow Chemical Co., Midland, MI), a typical gel-type poly(styrene-divinylbenzene) cation exchanger with a nominal divinylbenzene (DVB) content of 8% and sulfonic acid functional groups. The mean particle diameter of the hydrogen form resin is 714 μm, the dry weight is 0.48 g dry/g of hydrated resin, the bead density is 0.65 g dry/cm^3 of hydrated particle, and the total ion exchange capacity is 5.3 ± 0.2 mequiv/g dry H-form resin (1). L-lysine and other chemicals were obtained as described in Part I of this work. Feed solutions were prepared as described in Part I (1) from stock solutions of lysine hydrochloride and potassium chloride.

The experimental multicolumn system used in this study consists of five multiposition rotary valves, five high pressure liquid chromatography (HPLC) pumps, and eight columns. The arrangement used has the advantage of not requiring check valves. Instead, the five multiposition valves obtained from Valco Instruments Co., Inc. (Houston, TX, Model ECSTF8MWEHC) provide the distribution of lysine feed, rinse water, ammonia desorbent, and acid addition streams. The valves have eight pairs of matched ports plus one output and one input part, each connectable to any one of the eight matched port pairs. The matched ports that are not connected to input and output lines are connected to each other. The valves and columns were arranged as shown schematically in Fig. 2. Additional details can be found in Nagai (15).

The columns were 1.5 cm I.D., 10 cm long (Spectrum Chromatography, Houston TX; Model No. 123952) glass chromatography columns. They were packed with identical amounts of resin and connected to the valve system with 0.020″ ID PEEK tubing. Five HPLC pumps from LabAlliance (State College, PA, Series II Pump) were used to supply feed, rinse water streams, desorbent, and acid adsorption streams. The effluent streams were connected to fraction collectors (Gilson, Model 201) for off-line HPLC analysis as described in Nagai and Carta (1). An LKB Model 2195-100 pH/conductivity meter (Bromma, Sweden) was used online to monitor one of the effluent streams and help determine the attainment of steady state. The mV signal from this monitor was collected with a data acquisition system (Keyence, Osaka, Japan, Model NR-250) and logged on a PC. Switching of

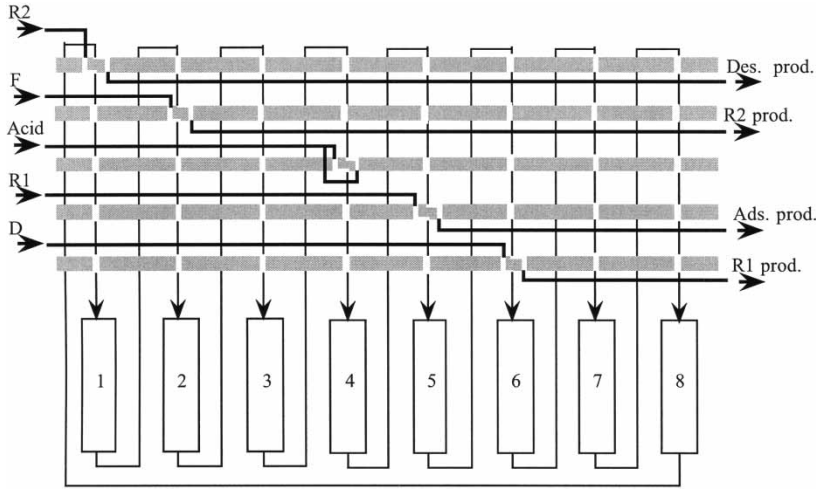

Figure 2. Schematic of experimental apparatus for multicolumn lysine recovery process. For clarity the five rotary valves are shown in a linearized form. Operation according to scheme C is shown with column 1 in the R2 zone, columns 2, 3, and 4 in the adsorption zone, column 5 in the R1 zone, and columns 6, 7, and 8 in the desorption zone. The effluent from column 3 is acidified before feeding it to column 4.

the valves was performed with electrically operated actuators controlled by a PLC (Keyence, Osaka, Japan, Model KV-700). Most of the dead volume in the system is from the tubing connected columns and valves. This volume was determined to be approximately 0.32 cm^3 per column or approximately 2% of the column volume. Because of the small value, no dead volume correction was deemed necessary.

MODEL DEVELOPMENT

The model used to simulate lysine recovery in the multicolumn systems is based on conservation equations for total lysine, total ammonia, potassium ion, and chloride ion and comprises the following components developed in our prior work (1, 2).

1. **Solution equilibria**. The equilibrium between divalent and monovalent cationic lysine, zwitterionic lysine, and anionic lysine and the equilibrium between ammonium ion and ammonia is expressed in terms of mass action law relationships using known values of the dissociation constants. The concentrations of charged species are bound by the electroneutrality condition, including dissociation of water into hydrogen ion

and hydroxyl ion. Since the concentrations of charged lysine species and ammonium ion can be expressed in terms of total lysine, $C_L = C_{Lys^{++}} + C_{Lys^{+}} + C_{Lys^{\pm}} + C_{Lys^{-}}$, total ammonia, $C_N = C_{NH_4^+} + C_{NH_3}$, and hydrogen ion concentration, the latter can be calculated from the electroneutrality condition if C_L, C_N, C_{K^+}, and C_{Cl^-} are known. These relationships are given in, Eqs. 9–13, in Part I of this work (1).

2. **Ion exchange and sorption equilibria**. The ion exchange of divalent and monovalent cationic lysine, ammonium ion, potassium ion, and hydrogen ion is described in terms of mass action law relationships using selectivity coefficients determined experimentally for binary pairs. The relevant equations, Eqs. 1–5, are given in Part I of this work (1). We neglect sorption of zwitterionic lysine and anions, an assumption validated experimentally. However, partitioning of NH_3 in the resin phase needs to be considered. This is important in the desorption step, since NH_3 is the dominant species in the concentrated ammonia solutions used in this work. The partition coefficient for NH_3 was obtained in Part II of this work (2). It should be noted that the concentrations of divalent and monovalent lysine and the concentration of ammonium ion and NH_3 are related by the corresponding dissociation equilibria. Values of the corresponding dissociation constants for the resin phase were determined in our prior work (1, 2).
3. **Mass transfer relationships.** Counter diffusion in the resin phase is described by the Nernst-Planck model equations. Counterion diffusivities were determined by matching single component batch uptake experiments with the Nernst-Planck model. This model is, however, computationally too demanding for column calculations, particularly those involving multicolumn systems. Thus, a simpler rate model based on the film model approximation of Carta and Lewus (16) is used to describe mass transfer rates. The relevant equations were obtained in Part II and are given by Eqs. 14–16 and 30–33 (2).
4. **Conservation equations.** Conservation equations are written for total lysine, total ammonia, potassium ion, and chloride ions assuming plug flow and neglecting axial dispersion. The relevant equations are given in Part II, Eqs. 1–2 and 11 (2). The axial derivatives are discretized by finite differences and the resulting system of ordinary differential equations is integrated simultaneously for all columns with the appropriate inlet conditions. The composition of the feed streams and initial resin phase compositions are assigned at the start of the simulation and the equations are integrated while material balances are solved where streams are mixed. At the end of a period the column concentration profiles are reassigned and the process is repeated until a periodic steady state is attained. For this condition, overall material balances for total lysine, total ammonia, potassium ion, and chloride ion are checked to be within $\pm 0.1\%$. The number of switches required to obtain a

periodic steady state varied from run to run. Generally, it was larger for smaller switch times and lower flow rates. Starting the simulation with all clean columns required anywhere between 20 and 30 switches.

EXPERIMENTAL RESULTS AND MODEL PREDICTIONS

The multicolumn apparatus described previously was used to validate the model. Experiments were conducted for the configurations shown in Fig. 1. Scheme A is an open loop configuration without ammonia recycle or acid addition. Scheme B includes a recycle of ammonia while scheme C includes an additional acid stream in the adsorption zone. In each case, the operational specifications include the number of columns in each stream, the switch time, and the column flow rates. A total of 10 experimental runs were performed with the conditions listed in Table 1. In all cases, the feed was a 0.20 M lysine hydrochloride solution (containing 0.2 M lysine and 0.2 M chloride ion). Monovalent lysine is the dominant form of lysine in these solutions (1). The desorbent is 1.0 M ammonia in water, while the rinse streams are distilled de-ionized water. Runs 1–5 are for scheme A, Runs 6–7 for scheme B, and Run 8 for scheme C. Runs 9 and 10 are for scheme A and C, respectively, but with the inclusion of potassium chloride in the feed with a 0.05 M concentration. A 3–1–3–1 scheme with three columns in the adsorption zone, one in the first rinse zone, three in the desorption zone, and one in the second rinse zone was used for all three schemes. Experimentally, the pH of the effluent from the desorption zone was monitored to confirm the achievement of steady state. After reaching steady state, 20 to 40 samples were collected from the effluent from each zone and analyzed by HPLC.

Representative experimental results at steady state are given in Figs. 3–8. In these figures the concentration profiles are shown as a function of RV, which is the effluent volume divided by the column volume, for the duration of one switch period. In each case, experimental profiles are compared with model predictions using the parameters summarized Part II of this work (2). Figure 3 shows the effluent profiles for a low flow rate case with scheme A where the switch time chosen was short enough to prevent breakthrough of lysine from the adsorption train but long enough to bring the lysine concentration in the desorption train near zero. Lysine is recovered from the desorption train in free-base form accompanied by a high ammonia concentration. However, it should be noted that the excess ammonia can be recovered readily by evaporation. The maximum lysine concentration in the desorption effluent is around 0.4 M, while the average is around 0.2 M, indicating that lysine recovery can be accomplished with essentially 100% yield and without dilution. Figure 4 shows the concentration profiles for the same configuration and switch time but with feed and R2

Table 1. Experimental conditions for multicolumn system[a]

Run No.	Scheme	C_L^F [M]	C_{K+}^F [M]	Switch time [s]	u_A [cm/s]	u_{RI} [cm/s]	u_D [cm/s]	u_{RI} [cm/s]
1	A	0.20	0	900	0.0072	0.0072	0.0072	0.0072
2	A	0.20	0	1,800	0.0072	0.0072	0.0072	0.0072
3	A	0.20	0	3,600	0.0072	0.0072	0.0072	0.0072
4	A	0.20	0	1,500	0.022	0.014	0.014	0.022
5	A	0.20	0	3,600	0.022	0.014	0.014	0.022
6	B	0.20	0	3,600	0.0072	0.0021	0.0051	0.0072
7	B	0.20	0	1,500	0.022	0.0041	0.010	0.022
8	C	0.20	0	3,600	0.022[b]	0.014	0.014	0.022
9	C	0.20	0.05	3,600	0.014[b]	0.014	0.014	0.014
10	A	0.20	0.05	3,600	0.014	0.014	0.014	0.014

[a] C_L^F and C_{K+}^F are the feed lysine hydrochloride and potassium chloride concentrations, u_i is the superficial velocity in zone i. The ammonia desorbent concentration was 1 M for all runs. All experiments were run in 3–1–3–1 scheme.

[b] u_A is the superficial velocity before acid addition. $u_A = 0.023$ and 0.015 cm/s after acid addition for Runs 8 and 9, respectively.

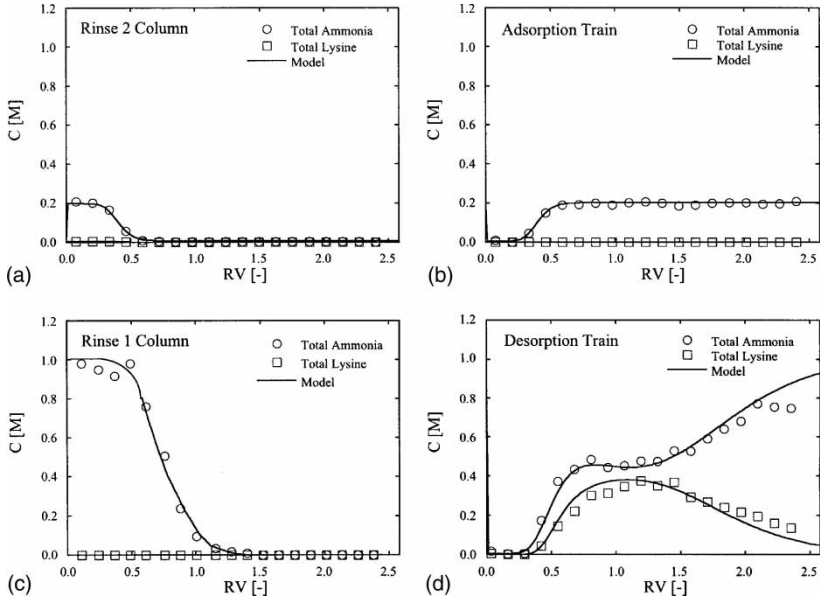

Figure 3. Comparison of experimental and predicted effluent profiles for Run 3 with scheme A and 3600 s switch time.

flow rates increased by a factor of 3 and desorbent and R1 flow rates increased by a factor of 2 relative to Fig. 3. Although the throughput has been increased by a factor of 3, the lysine yield in the desorption train effluent is no longer 100%. This occurs because the switch time is now too long and breakthrough of lysine occurs in the adsorption train. However, as a result of the greater loading of lysine on the resin in the adsorption train, a greater lysine concentration is attained, around 0.7 M. The tailing visible in Fig. 4 is a result of the slow diffusion of lysine in the resin phase. Figure 5 shows the results for Run 4, which had exactly the same conditions as those in Fig. 4 but a switch time of only 1500 s. As seen in this figure, the shorter switch time prevents breakthrough of lysine from the adsorption train. The maximum lysine concentration in the desorption effluent is around 0.45 M, but the average is now 0.3 M. The only yield loss of lysine occurs in the R2 rinse. This occurs because at the higher flow rate of this run, the first column in the adsorption train is nearly saturated with lysine so that some is lost when the void volume is swept by the R2 stream prior to desorption.

Figure 6 shows effluent concentration profiles for Run 7. The lysine feed flow rate and the switch time are the same as in Run 4 (Fig. 4). However, the system was the ammonia recovery scheme B. As a result, a lower ammonia desorbent flow rate is sufficient to attain essentially complete desorption. There is no breakthrough of lysine from the adsorption train and the yield is

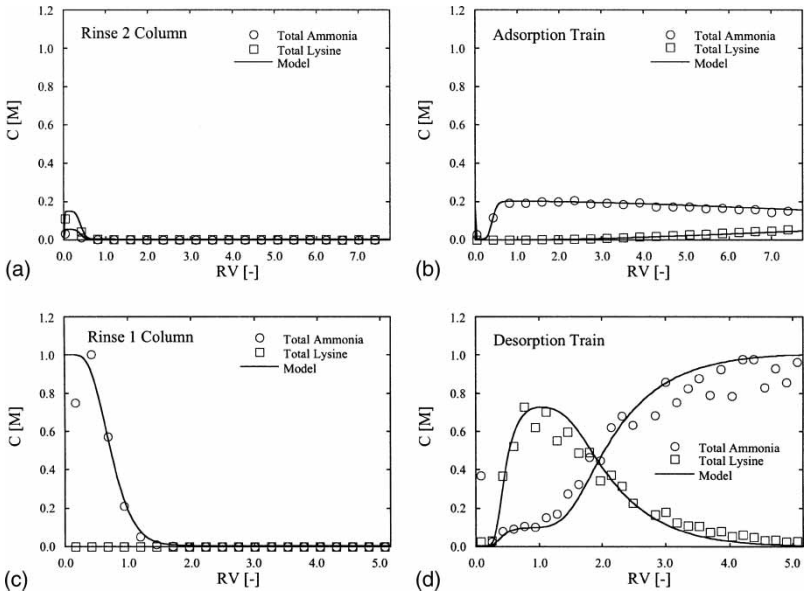

Figure 4. Comparison of experimental and predicted effluent profiles for Run 5 with scheme A and 3600 s switch time at high flow rate.

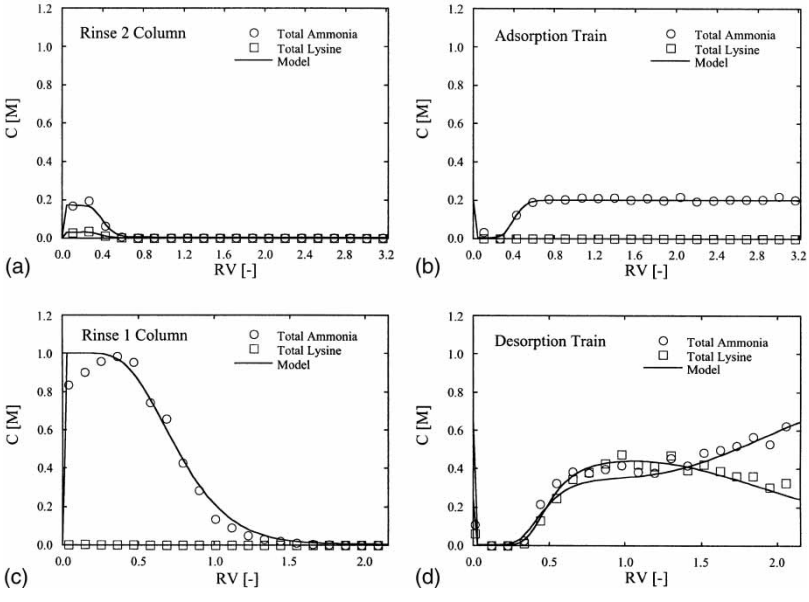

Figure 5. Comparison of experimental and predicted effluent profiles for Run 4 with scheme A. Conditions are the same as in Fig. 4 but with 1500 s switch time.

close to 100% except for the small lysine loss for RV < 0.4 (the column void fraction) in the R2 column. Comparing Figs. 5 and 6, it can be seen that for short times a relatively high ammonia concentration exists in the effluent of the adsorption train for Run 7 (Fig. 6). This occurs because a much lower rinse flow rate was used in this run so that not all of the excess ammonia from the desorption train was purged in position 4.

Figure 7 shows the profiles for Run 8, which involves acid addition to the third column in the adsorption train (scheme C). As discussed before, divalent lysine is favorably adsorbed and shows a steeper breakthrough curve because the ion exchange equilibrium favors divalent lysine that, in turn, generates a shock wave. Conversely, monovalent lysine results in a shallower

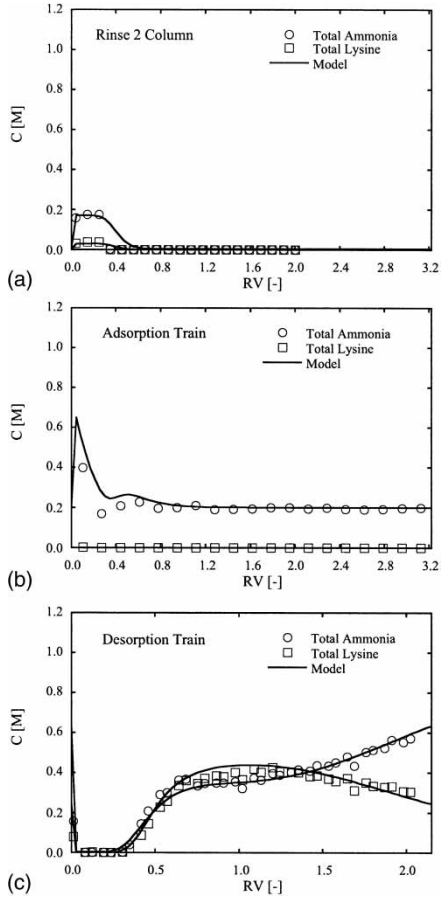

Figure 6. Comparison of experimental and predicted effluent profiles for Run 7 with ammonia recycle scheme B and 1500 s switch time.

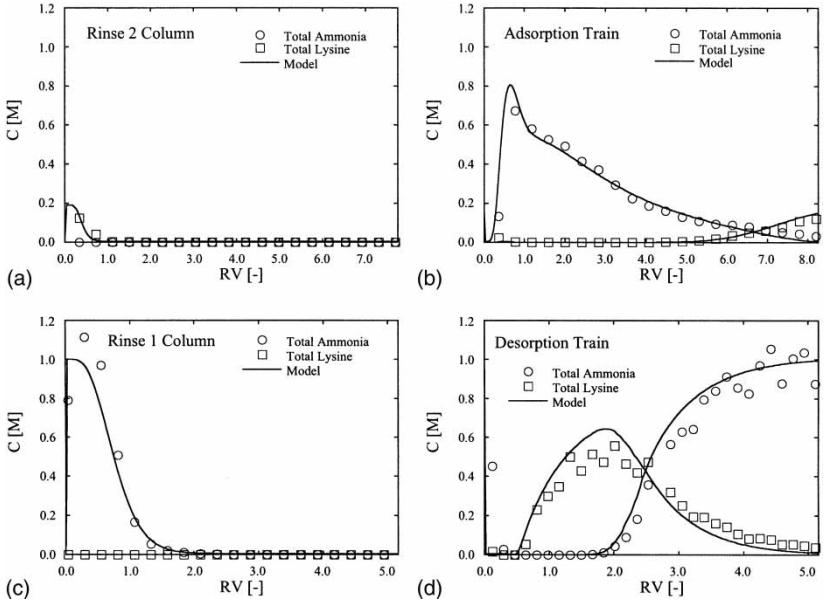

Figure 7. Comparison of experimental and predicted effluent profiles for Run 8 with acid addition scheme C and 3600 s switch time.

breakthrough because of the unfavorable nature of its ion exchange. However, the capacity of the resin for monovalent lysine is twice as large as that for divalent lysine. To prevent lysine leakage from the adsorption train while maintaining high capacity, acid can be added at an intermediate point in the adsorption train to convert monovalent lysine leaking through into divalent lysine as suggested in Van Walsen and Thompson (4). Accordingly, the last column in this train would function as a final capture or polishing bed. Conditions for this run are otherwise identical to those of Run 5 (Fig. 4). The predicted curves show good agreement with experimental data. However, contrary to expectations, the leakage of lysine in the adsorption train is actually larger than in Run 5. This difference is discussed in a later section.

Finally, Fig. 8 shows the results for Run 9 where the feed contains 0.05 M potassium chloride in addition to 0.20 M lysine hydrochloride. Inorganic ions in the fermentation broth media are significant impurities in the lysine feed stock. Thus, modeling their behavior is important. It can be seen that the behavior of potassium ion is accurately predicted. As discussed in our previous work (2), potassium ion is displaced by divalent lysine in acidic condition. Therefore, it breaks through unadsorbed at RV = 0.4 in the adsorption train. The lysine desorbed is thus essentially free of potassium ion. It can be noted that the leakage amount of lysine is less than that shown in Run 8

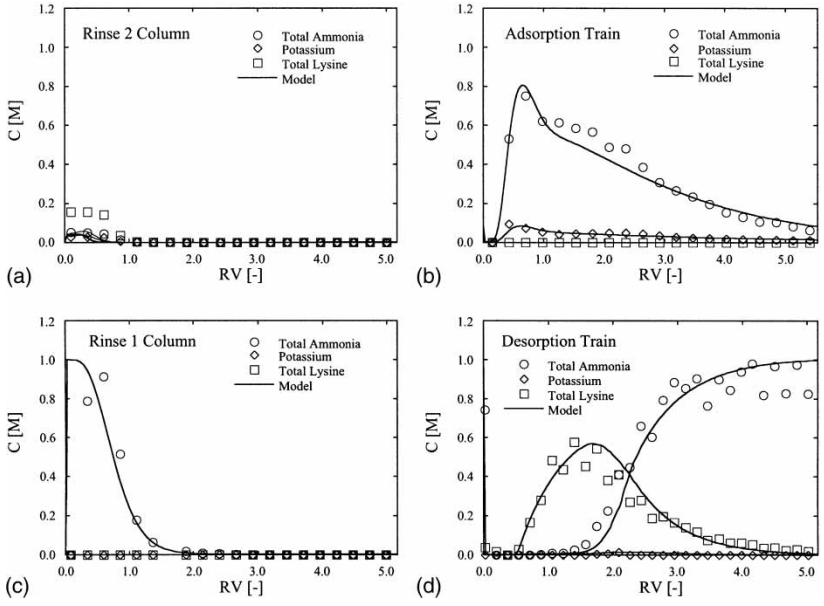

Figure 8. Comparison of experimental and predicted effluent profiles for Run 9 with acid addition scheme C. Conditions are as in Fig. 7 but with lower flow rates and 0.05 M potassium chloride in the lysine feed stream.

(Fig. 7) without potassium ion. However, this difference is not caused by the existence of potassium ion but by the lower feed flow rate used in Run 9.

PARAMETRIC STUDIES

As seen previously, the agreement with the experimental profiles was very good in all cases, suggesting that the model can be used as a tool to explore the effect of operating conditions beyond those investigated experimentally. A comprehensive optimization of the operation is beyond the scope of this work. However, in the following discussion we examine certain important effects.

The first effect considered is that of the number of columns and the switch time. For this study, we consider scheme A with a fixed amount of resin and different column numbers. The first case, 1–1–1–1, corresponds to four columns 20 cm long, the second, 3–1–3–1, corresponds to three columns in the adsorption zone, one in the R1 zone, three in the desorption zone, and one in the R2 zone, and so on. The results are shown in Fig. 9 in terms of the overall lysine recovery yield in the desorbent effluent. As seen in Fig. 9, the optimum switch time decreases as the number of columns is increased. When the switch time is too long, breakthrough occurs from the

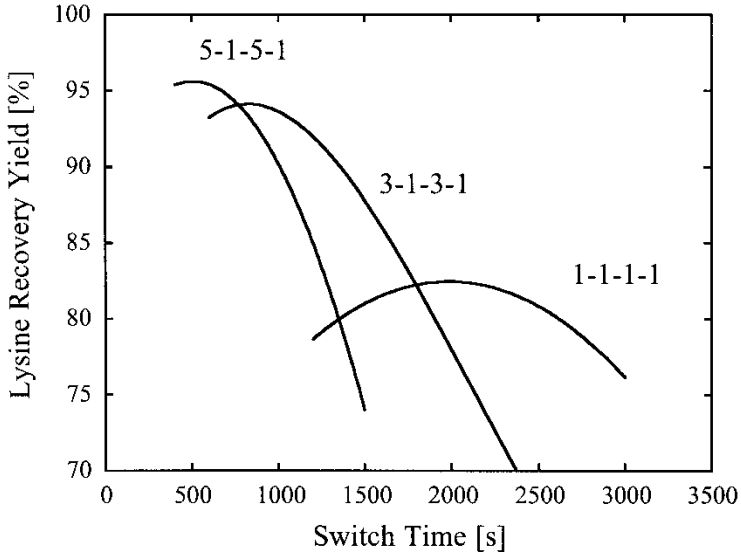

Figure 9. Simulated lysine recovery yield for scheme A with different number of columns while keeping the total column length constant. The superficial velocity for all zones is set at 0.043 cm/s.

adsorption train. Conversely, when the switch time is too short, an excessive amount of lysine is lost in the R1 effluent. It can be seen that most of the benefits are accrued with the first few subdivisions of the resin into multiple columns. Going beyond 12 total columns appears to yield diminished returns.

The second effect is the number of columns and the desorbent velocity in the desorption train. The results are shown in Fig. 10 in terms of the lysine yield loss in the R1 train. This gives the amount of lysine that we would loose because of incomplete desorption. For these calculations, the flow rate in the adsorption train and the switch time were kept constant. It can be seen that as the column number is increased, the minimum desorbent velocity needed to reduce the yield loss to zero decreases. However, there is not much difference between the 1–1–3–1 and the 1–1–4–1 configurations, and it appears that there is an absolute minimum desorbent velocity of 0.006 cm/s to reduce the yield loss to zero.

The third effect studied relates to the ammonia recovery scheme (scheme B in Fig. 1). Simulations were done for the 3–1–3–1 configuration with the velocity kept constant in all zones at 0.0072 cm/s, except in the R1 column. The effects of the ratio of R1 and D velocities are shown in Fig. 11. It appears that increasing the R1 flow rate reduces ammonia consumption. Up to a certain point, there is no effect on lysine yield. However, beyond that point, the lysine yield decreases substantially. This occurs when the amount

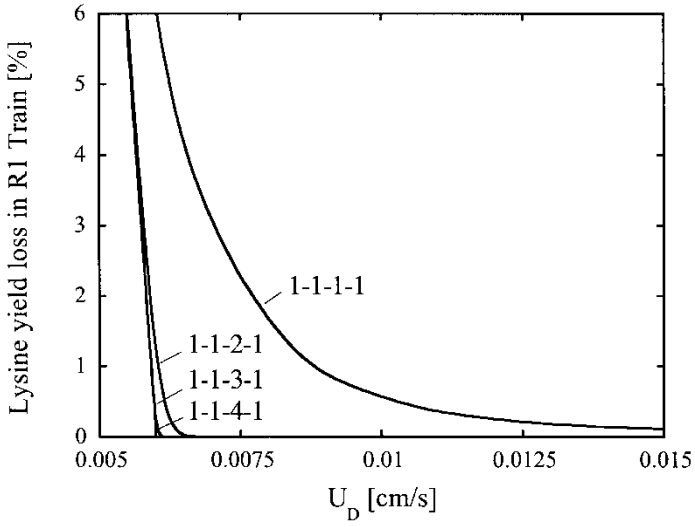

Figure 10. Simulated lysine yield loss for scheme A with a different number of columns in the desorption train. The superficial velocity for all zones except the desorption train is set at 0.022 cm/s. The switch time is 3600 s.

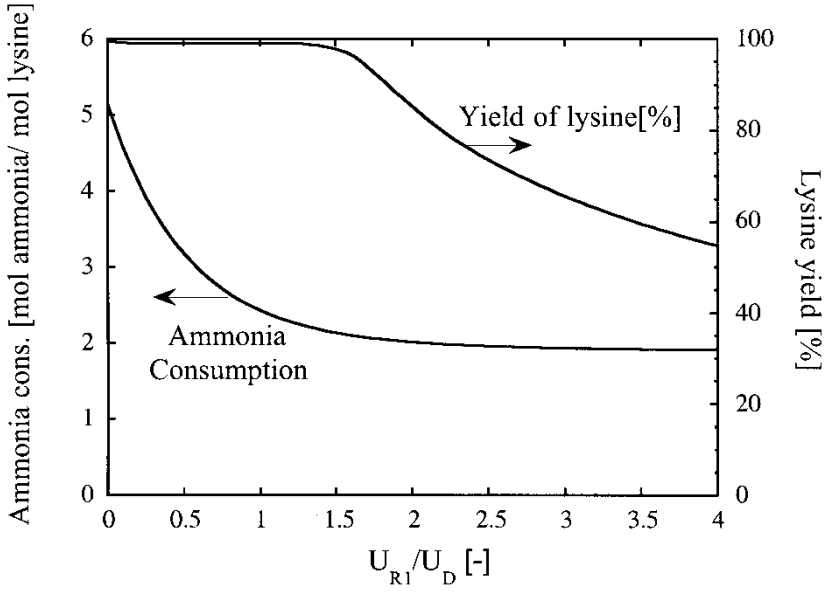

Figure 11. Simulated lysine recovery yield and ammonia desorbent consumption for ammonia recovery scheme B. The superficial velocity for all zones except the R1 column is set at 0.0072 cm/s. The switch time is 3600 s.

of ammonia fed is no longer sufficient to desorb lysine from the resin and leakage in the adsorption train becomes significant.

The last effect studied is the addition of acid to the end column in the adsorption train (scheme C). As previously discussed, it was suggested that lowering the pH could result in a greater dynamic binding capacity since at low pH lysine would be converted to the more favorably adsorbed divalent cationic form. The increase in dynamic binding capacity with lower pH was seen in the single column experiments discussed in Part II of this work (2). However, it was not seen for the multicolumn experiment in Fig. 7. To understand why this happened, simulations were done for the 3–1–3–1 scheme C by varying the velocity in the adsorption zone. The results are shown in Fig. 12 in terms of the lysine yield loss in the adsorption train effluent. It can be seen that at high velocities, acid addition actually yields greater losses. Conversely, at low velocities acid addition results in a significant reduction of lysine loss. This behavior can be explained as follows. While divalent lysine is favorably adsorbed resulting in a shock wave, the capacity is lower than it is for monovalent lysine. Moreover, the diffusivity of divalent lysine is substantially smaller than is that for the monovalent form. As a result, at high flow rates, when the system is far from equilibrium, the lower adsorption capacity for the divalent form results in an earlier breakthrough. Conversely, at low flow

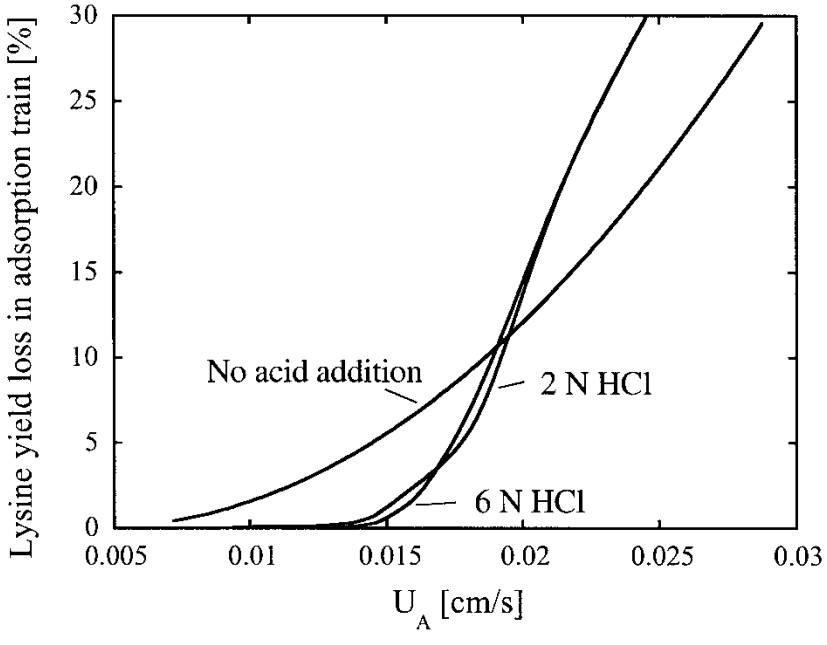

Figure 12. Simulated lysine recovery yield for acid addition scheme C. The superficial velocity is set equal for all zones.

rates, the sharper wave behavior of divalent lysine results in a longer breakthrough time compared to the monovalent form. The experiment in Fig. 7 was for a velocity of 0. 021 cm/s. As seen in Fig. 12, for this velocity we expect the no acid addition case to yield better performance.

CONCLUSIONS

The single column model for lysine adsorption and desorption developed in our previous work (2) was extended to the description of a continuous multicolumn ion exchange process. The multicolumn system includes a zone for lysine adsorption and one for lysine desorption, as well as intermediate zones to remove unadsorbed components and excess desorbent, with each zone comprising multiple columns in a simulated countercurrent arrangement. Three cases were considered. In the first, there are no recycle or addition streams so that each zone is coupled only by the periodic switching of columns in a merry-go-round sequence. In the second case, the stream leaving the Rinse 1 zone is mixed with the desorbent feed and recycled, while keeping the same merry-go-round switching of columns. This configuration allows recycling of the excess ammonia present in the columns at the end of a period and reduces the desorbent consumption. In the third case, the same merry-go-round sequence is used. However, prior to entering the last column in the adsorption train, the liquid is acidified to convert lysine to the divalent form, thereby sharpening the breakthrough curve. Lysine hydrochloride solutions are fed to the process with the product being lysine in free-based form. In all three cases, the model was found to be in agreement with experimental results obtained in a bench scale apparatus comprising a total of eight columns. Then, the model was employed to survey the effects of various operating parameters. Firstly, the effect of the simulated counter current motion was tested by changing the number of columns while using constant of resin. The yield of lysine increases as the number of columns in series is increased. However, while there was a large improvement increasing the number of columns from one to two, subsequent increases had a smaller effect. Secondly, the use of multiple columns for desorption was examined. Compared to single column operation, the multicolumn process shows a reduction in the consumption of ammonia by increasing the number of columns in the desorption train. Thirdly, ammonia recovery by recycling the Rinse 1 effluent was shown to reduce the ammonia consumption to one half of the case without ammonia recovery. Lastly, the effects of acid addition on lysine recovery yield were investigated. It was found that the acid addition could prevent the leakage of lysine from the adsorption train up to a certain flow rate beyond which acid addition becomes counterproductive.

REFERENCES

1. Nagai, H. and Carta, G. (2004) Lysine adsorption on cation exchange resin I. Ion exchange equilibrium and kinetics. *Sep. Sci. Technol.*, in review.
2. Nagai, H. and Carta, G. (2004) Lysine adsorption on cation exchange resin II. Column adsorption/desorption behavior and modeling. *Sep. Sci. Technol.*, 39: 3691–3710.
3. Rossiter, G.J. and Tolbert, C.A. (1991) *Recovery of Amino Acids and Carboxylic Acids by Continuous Exchange*; AIChE Annual Meeting: Los Angeles, CA, November.
4. Van Walsem, H.J. and Thompson, M.C. (1997) Simulated moving bed in the production of lysine. *J. Biotechnol.*, 59: 127–132.
5. Broughton, D.B. (1968) Molex: case history of a process. *Chem. Eng. Progr.*, 64: 60–65.
6. Rearick, D.E., Kearney, M., and Costesso, D.D. (1997) Simulated moving bed technology in the sweetener industry. *Chem. Tech.,* Sept., 36–40.
7. Wu, D.-J., Xie, Y., Ma, Z., and Wang, N.-H.L. (1998) Design of simulated moving bed chromatography for amino acid separations. *Ind. Eng. Chem. Research.*, 37: 4023–4035.
8. Kinkel, J.N., Schulte, M., Nicoud, R.M., and Charton, F. (1995) Simulated moving bed (SMB) chromatography: An efficient method for performing large scale separation of optical isomers? Proceedings of Chiral Europe '95 Symposium, Spring Innovations Limited: Stockport, UK, 121.
9. Gattuso, M.J. (1995) UOP sorbex simulated moving bed (SMB) technology. A cost-effective route to optically pure products. *Chim. Oggi*, 13: 18–22.
10. Schulte, M. and Strube, J. (2001) Preparative enantioseparation by simulated moving bed chromatography. *J. Chromatogr. A*, 906: 399–416.
11. Ruthven, D.M. and Ching, C.B. (1989) Counter-current and simulated counter-current adsorption separation processes. *Chem. Eng. Sci.*, 44: 1011–1038.
12. Storti, G., Mazzotti, M., Morbidelli, M., and Carrá, S. (1993) Robust design of binary countercurrent adsorption separation processes. *AIChE J.*, 39: 471–492.
13. Ma, Z. and Wang, N.-H.L. (1997) Design of simulated moving bed chromatography using standing wave analysis: linear systems. *AIChE J.*, 43: 2488–2508.
14. Antia, F.D. (2003) A simple approach to design and control of simulated moving bed chromatographs. In *Scale-Up and Optimization in Preparative Chromatography—Principles and Biopharmaceutical Applications*; Rathore, A.S. and Velayudhan, A., Eds.; Marcel Dekker: New York, 173–201.
15. Nagai, H. (2003), Ph.D. Thesis. University of Virginia: Charlottesville, Virginia.
16. Carta, G. and Lewus, R.K. (1999) Film model approximation for particle-diffusion-controlled multicomponent ion exchange. *Sep. Sci. Technol.*, 34: 2685–2697.